

# CMB anisotropy induced by tachyonic perturbations of dark energy

M.V. Libanov<sup>†</sup>, V.A. Rubakov<sup>‡</sup>, O.S. Sazhina<sup>\*</sup> and M.V.Sazhin<sup>\*</sup>

<sup>†</sup> Institute for Nuclear Research of the Russian Academy of Sciences,  
60th October Anniversary Prospect, 7a, Moscow, Russia;

<sup>\*</sup> P.K. Sternberg Astronomical Institute of the Moscow State University,  
Universitetsky Prospect, 13, Moscow, Russia.

May 29, 2019

## Abstract

We study effects of possible tachyonic perturbations of dark energy on the CMB temperature anisotropy. Motivated by some models of phantom energy, we consider both Lorentz-invariant and Lorentz-violating dispersion relations for tachyonic perturbations. We show that in the Lorentz-violating case, the shape of the CMB anisotropy spectrum generated by the tachyonic perturbations is very different from that due to adiabatic scalar perturbations and, if sizeable, it would be straightforwardly distinguished from the latter. The tachyonic contribution improves slightly the agreement between the theory and data; however, this improvement is not statistically significant, so our analysis results in limits on the time scale of the tachyonic instability. In the Lorentz-invariant case, tachyonic contribution is a rapidly decaying function of the multipole number  $l$ , so that the entire observed dipole can be generated without conflicting the data at higher multipoles. On the conservative side, our comparison with the data places limit on the absolute value of the (imaginary) tachyon mass in the Lorentz-invariant case.

## PACS:

98.80.-k, 95.36.+x

# 1 Introduction

Recently, a number of suggestions have been put forward for explaining the observed accelerated expansion of the Universe. Among them there are the presence of the cosmological constant, modification of gravity at ultra-large scales, existence of new light fields (for reviews, see, e.g., Refs. [1, 2, 3, 4, 5]). In the latter case, dark energy can be characterized by equation of state  $p = w\rho$ , where the parameter  $w$  is different from  $-1$  and generically depends on time. In a simple version, dark energy is due to a scalar field (quintessence), and the parameter  $w$  obeys the constraint  $w > -1$ , while  $w = -1$  for the cosmological constant. However, the value of  $w$  may be strongly negative,  $w < -1$ ; this is the case for phantom dark energy. Existing data do not exclude also a possibility [6, 7, 8] that at relatively large redshift the dark energy is of quintessence type,  $w > -1$ , and later it becomes phantom with  $w < -1$ .

Phantom energy violates null energy condition, which is usually a signal for instabilities. As an example, the simplest model of scalar field with wrong sign of kinetic term [9] suffers from the presence of ghost (negative energy state) at arbitrarily high spatial momenta. This implies catastrophic vacuum instability. However, in phantom models that break Lorentz-invariance, violation of null energy condition at cosmological scales (related to the property that  $w < -1$  for spatially homogeneous phantom field) does not necessarily imply unacceptable instabilities at shorter scales. This suggests that Lorentz-violating phantom theories may be viable. Indeed, models of this sort have been recently constructed [10, 11, 12, 13]. A property of one class of these models [12, 13] is that there is a tachyonic mode in the perturbation spectrum about the homogeneous phantom background. This mode occurs at sufficiently small spatial momenta only, so that the time scale of the tachyonic instability may be roughly comparable to the age of the Universe. This is not particularly dangerous.

It is conceivable that the existence of tachyonic modes at low spatial momenta is a fairly generic property of a class of phantom models: the violation of the null energy condition may show up precisely in this way. Therefore, it is of interest to study observable consequences of such models. In this paper we consider one of these consequences, namely, the effect of tachyonic modes on the anisotropy of CMB temperature. We adopt the phenomenological approach, and instead of using results obtained within a concrete model, we parametrize the tachyonic instability by a few parameters. We will consider in parallel models with Lorentz-violating dispersion relation and Lorentz-invariant one.

In the Lorentz-violating case, we parametrize the dispersion relation as follows,

$$\omega^2 = \alpha|\mathbf{p}|(M - |\mathbf{p}|), \tag{1}$$

where  $\alpha$  and  $M$  are constant parameters, and  $\mathbf{p}$  is the physical spatial momentum. Our convention is that positive values of  $\omega^2$  correspond to exponential growth of perturbations, while the usual oscillatory behaviour occurs at negative  $\omega^2$ . Thus, the parameter  $M$  equals

to the momentum below which the mode is tachyonic. For given  $\alpha$ , the parameter  $M$  determines also the time scale of instability. The parametrization (1) is chosen in accord with Refs. [12, 13] where similar dispersion relation has been found in a concrete model of phantom energy. The analysis presented below can be straightforwardly generalized to other forms of dispersion relation.

In the Lorentz-invariant case the dispersion relation has the form

$$\omega^2 = M^2 - \mathbf{p}^2 \quad (2)$$

In this case too, the tachyon mass  $M$  equals to the spatial momentum below which the mode is unstable, and  $M^{-1}$  is the time scale of instability. From our prospective, the important difference between the dispersion relations (1) and (2) is that in the latter case the “frequency” is non-zero at  $\mathbf{p} = 0$  and monotonously decreases as  $|\mathbf{p}|$  increases, whereas in the former, the “frequency” vanishes as  $\mathbf{p} = 0$  and has a maximum at finite  $|\mathbf{p}|$ . This will lead to qualitatively different shapes of the contributions to the CMB anisotropy spectra. It is worth noting in this regard that the Lorentz-invariant model may be viewed as a representative of a class of theories with tachyonic perturbations: analogous results would hold for Lorentz-violating models with dispersion relations similar to (2).

In the cosmological context, the dispersion relations (1) and (2) are written as follows,

$$\begin{aligned} \omega^2(t) &= \alpha \frac{k}{a(t)} \left( M - \frac{k}{a(t)} \right), \\ \omega^2(t) &= M^2 - \frac{k^2}{a^2(t)}, \end{aligned}$$

respectively, where  $k$  is time-independent conformal momentum and  $a(t)$  is the scale factor. In the expanding Universe, a mode of given  $k$  is first normal, and after the physical momentum gets reshifted down to  $k/a = M$ , it becomes unstable.

For  $M > H_0$ , where  $H_0$  is the present value of the Hubble parameter, the tachyonic modes in both models start to grow exponentially at times preceding the present cosmological epoch. The growth of the tachyonic perturbations gives rise to the growth of the gravitational potential  $\Phi$  generated by these perturbations<sup>1</sup> [14]

$$\begin{aligned} \Phi(t, \mathbf{x}) &= \frac{1}{(2\pi)^{3/2}} \int d\mathbf{k} \Phi(t, \mathbf{k}) e^{i\mathbf{k}\mathbf{x}} + \text{h.c.}, \\ \Phi(t, \mathbf{k}) &= A(\mathbf{k}) \exp \left( \int_{t_k}^t \omega(t') dt' \right), \end{aligned} \quad (3)$$

---

<sup>1</sup>Refs. [13, 14] consider Lorentz-violating case, but that analysis is straightforwardly repeated in the Lorentz-invariant situation.

where  $A(\mathbf{k})$  is the amplitude of vacuum fluctuations in the mode with conformal momentum  $\mathbf{k}$  at the time  $t_k$  when this mode becomes unstable. We will estimate the amplitude  $A(\mathbf{k})$  later on. We stress that the gravitational potential (3) is generated by tachyonic perturbations rather than inhomogeneities in the ordinary matter.

In this paper we calculate CMB multipoles generated by the gravitational potential (3). In the Lorentz-violating case, the mechanism we discuss gives rise to the contribution to the CMB anisotropy spectrum which is quite different from the standard spectrum coming from adiabatic scalar perturbations generated, e.g., at inflationary stage (for the latter see, e.g., Refs. [15, 16, 17]). As we will see below, the tachyonic contribution leads to potentially observable features in the CMB spectrum at relatively low multipoles. On the other hand, there are hints towards the existence of deviations in the observed spectrum [6, 18] from the predictions based on flat (Harrison–Zeldovich) or almost flat spectrum of primordial adiabatic perturbations. So, one is tempted to employ tachyonic instabilities for explaining these deviations. We add the contribution due to the tachyonic perturbations to the standard contribution of the adiabatic modes and compare the result with the observed spectrum. We show that the tachyonic contributions slightly improve the agreement between the theory and data, but this improvement is statistically insignificant. So, our analysis only leads to limits on the parameters of the tachyonic perturbations.

In the Lorentz-invariant case, tachyonic perturbations contribute to the lowest multipoles only. An interesting possibility here is that they may generate the entire observed dipole without getting in conflict with measurements of higher multipoles.

This paper is organized as follows. We begin with preliminaries on the cosmological model in section 2, and then discuss in detail the growth of the gravitational potential due to the tachyonic modes in section 3, first in the Lorentz-violating model and then in the Lorentz-invariant one. In section 4 we calculate the contributions to the CMB multipoles, again distinguishing Lorentz-violating and Lorentz-invariant cases. We compare our results with the data in section 5, and conclude in section 6.

## 2 The cosmological model

The background space-time we consider in this paper corresponds to “almost” standard cosmological model with the only special feature that the accelerated expansion of the Universe is driven by phantom energy instead of the cosmological constant. The background metric is that of the spatially flat expanding Universe,

$$ds^2 = dt^2 - a^2(t)d\mathbf{x}^2.$$

The scale factor  $a(t)$  is determined by the Friedmann equation, which can be written as follows,

$$\left(\frac{\dot{a}(t)}{a(t)}\right)^2 = H_0^2 \left[ \Omega_m \left(\frac{a(t_0)}{a(t)}\right)^3 + \Omega_p \left(\frac{a(t)}{a(t_0)}\right)^{-3(1+w_p)} \right], \quad (4)$$

where  $H_0$  is the present value of the Hubble parameter,  $a(t_0) = a_0 = 1$  is the present value of the scale factor, dot denotes the derivative with respect to cosmic time  $t$ ,  $\Omega_p$  and  $w_p$  refer to phantom energy. We assume for simplicity that  $w_p \equiv p_p/\rho_p$  is independent of time; we will see in what follows that the effects we discuss are largely independent of  $w_p$ , so this assumption is not restrictive. The values we use in this paper are  $\Omega_m = 0.27$ ,  $\Omega_p = 0.73$ . According to observational data [6] the parameter  $w_p$  belongs to the interval  $-1.38 < w_p < -0.86$ .

When calculating the CMB multipoles, we work with conformal time  $\eta$  instead of cosmic time  $t$ ,

$$\eta(t) = \int_0^t \frac{d\hat{t}}{a(\hat{t})}.$$

Equation (4), written in terms of conformal time, has the form

$$H_0 d\eta = \frac{da}{\sqrt{a} \sqrt{\Omega_m + \Omega_p a^{-3w_p}}}.$$

### 3 Growth of perturbations

The gravitational potential of a mode in the tachyonic regime is given by eq. (3). The exponent

$$N(t, k) = \int_{t_k}^t d\hat{t} \omega(\hat{t}) \quad (5)$$

determines the growth of the potential in both Lorentz-violating model (1) and Lorentz-invariant one (2). Properties of this function are different in the two cases, however.

#### 3.1 Lorentz-violating model.

In the Lorentz-violating model, the function (5) can be written as an integral over the scale factor,

$$N(a, k) = \sqrt{\alpha} \frac{M}{H_0} \sqrt{\nu} \int_{a_k}^a d\hat{a} \frac{\sqrt{\hat{a} - \nu}}{\sqrt{\hat{a}} \sqrt{\Omega_m + \Omega_p \hat{a}^{-3w_p}}}, \quad (6)$$

where we have introduced dimensionless wave number

$$\nu = \frac{k}{M}.$$

A few comments are in order. First, for a given mode the tachyonic regime begins when the integrand in (6) becomes real, i.e., at  $a = \nu$ . Since  $a \leq a_0 = 1$ , the maximum value of  $\nu$  for tachyonic modes is  $\nu = 1$ , that corresponds to the modes that are entering the tachyonic regime today. In fact, because of the Hubble friction, the exponential growth of the tachyonic mode starts slightly later than  $a$  reaches  $\nu$ , namely, at the time  $t_k$  when the tachyonic “frequency” becomes comparable to the Hubble parameter,

$$\omega(t_k) \simeq H(t_k). \quad (7)$$

The lower limit of integration in (6) is the value of the scale factor at that time,  $a_k = a(t_k)$ .

Second, the integral in (6) is a dimensionless smooth function of its arguments  $\{a, \nu\}$ , both of which do not exceed 1. Therefore, this integral is not parametrically large or small. On the other hand, the amplitude  $A(\mathbf{k})$  is small (see below), so the effect of the tachyonic instability may be considerable only if  $N(a, k)$  is sufficiently large. This can happen if

$$\sqrt{\alpha}M > H_0. \quad (8)$$

We assume in what follows that this inequality is indeed valid.

Third, the integral in (6) is saturated near its upper limit, and because of (8) this integral is practically insensitive to the lower limit of integration. Therefore, it is an excellent approximation to set  $a_k = \nu$ , that is, approximate the time  $t_k$  by the time at which the dispersion relation becomes tachyonic. In fact, by solving eq. (7) numerically, we have found that  $a_k = \nu$  with precision of order  $10^{-5}$  in a wide range of values of  $\nu$  ( $1 \geq \nu \geq 0.05$ ). By setting  $a_k = \nu$  in (6) one finds that the dependence of  $N$  on the parameters  $M$  and  $\alpha$  factors out,

$$\begin{aligned} N(a, \nu) &= \sqrt{\alpha} \frac{M}{H_0} \mathcal{N}(a, \nu), \\ \mathcal{N}(a, \nu) &= \sqrt{\nu} \int_{\nu}^a d\hat{a} \frac{\sqrt{\hat{a} - \nu}}{\sqrt{\hat{a}} \sqrt{\Omega_m + \Omega_p \hat{a}^{-3w_p}}}. \end{aligned}$$

Fourth, the function  $\mathcal{N}(a, \nu)$  is obviously a growing function of the scale factor  $a$ , as shown in the left panel of Fig. 1. This is especially relevant since the gravitational potential (3) depends on  $N$  exponentially. We present in the right panel of Fig. 1 the dependence of  $\exp[N(a, \nu)]$  on the scale factor at  $\nu = 0.2$ ; the plot is given for the values of parameters<sup>2</sup> such that  $\sqrt{\alpha}M/H_0 = 100$ . It is clear that the major effect of tachyonic modes occurs at late times.

Finally, let us discuss the dependence of  $\mathcal{N}(a, \nu)$  on the parameter  $w_p$ . We show in Fig. 2 the function  $\mathcal{N}(a, \nu)$  at  $a = 1$  for different values of this parameter. Clearly, the dependence on  $w_p$  is weak; in what follows we take  $w_p = -1$  for definiteness.

---

<sup>2</sup>The effect of the tachyonic instability on the CMB anisotropy is sizeable if  $\sqrt{\alpha}M/H_0 \sim 100$  (see section 5.2), hence our choice here.

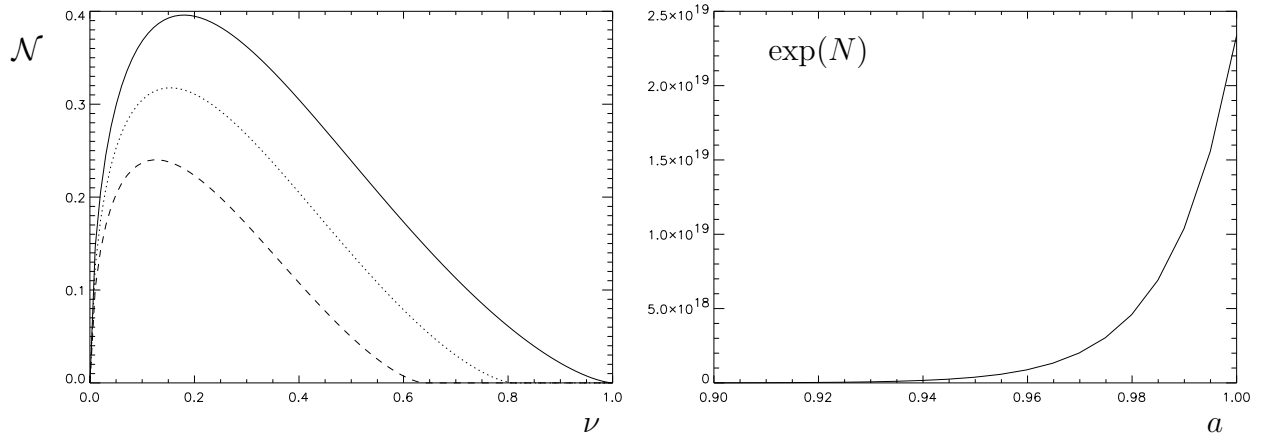


Figure 1: **Left:** The growth function  $\mathcal{N}(a, \nu)$  as a function of  $\nu$  at the values of the scale factor  $a = 0.8$ ,  $a = 0.9$  and  $a = 1.0$  (dashed, dotted and solid lines, respectively). Clearly,  $\mathcal{N}$  has a maximum at  $\nu \simeq 0.2$  and grows considerably as the scale factor approaches its present value  $a = 1$ . **Right:** The growth factor  $\exp[N(a, \nu)]$  as a function of the scale factor  $a$  at  $\nu = \nu_{\max} \simeq 0.2$ . The function  $\exp[N(a, \nu)]$  becomes comparable to its present value only at  $a \gtrsim 0.95$ . Calculations are done for  $w_p = -1$ ,  $\sqrt{\alpha}M/H_0 = 100$ .

The growth function  $\mathcal{N}(a, \nu)$  as a function of  $\nu$  has a pronounced maximum at  $\nu_{\max} = 0.2$ . The existence of a maximum of  $\mathcal{N}(a, \nu)$  is a fairly generic property independent of the particular form of the parametrization (1), provided that  $\omega(\mathbf{p})$  vanishes at  $\mathbf{p} = 0$ . Indeed, the tachyonic regime begins at  $k/a(t) = M$ . This implies, in particular, that  $\mathcal{N}(a, \nu)$  vanishes at  $\nu = 1$ . Now, under the assumption that  $\omega(\mathbf{p} = 0) = 0$  one observes that  $\mathcal{N}(a, \nu)$  vanishes at  $\nu = 0$  as well. Hence,  $\mathcal{N}(a, \nu)$  has a maximum at some intermediate  $\nu$ . In other words, modes of high conformal momenta have not entered the tachyonic regime yet. On the other hand,  $\mathcal{N}(a, \nu)$  is small also at low conformal momenta, since the tachyonic regime begins too early for the corresponding modes. At that time the scale factor increases too rapidly; the function  $\mathcal{N}(a, \nu)$  does not have enough time to grow by the epoch when the physical momentum  $k/a(t)$  gets close to zero and the growth terminates. The maximum growth occurs for intermediate momenta. We note in passing that the situation is different in the Lorentz-invariant model (2), since in that case  $\omega(\mathbf{p} = 0) = M \neq 0$ , and the maximum growth takes place at the lowest spatial momenta.

Besides the growth function  $N$ , the gravitational potential (3) is determined by the amplitude  $A(\mathbf{k})$  at the time the perturbations enter the tachyonic regime. So, we have to estimate this amplitude at  $k/a = M$ . We assume that the tachyonic perturbations start off as vacuum fluctuations. Hence, the amplitude is the Gaussian random field with zero expectation value,  $\langle A(\mathbf{k}) \rangle = 0$ . This field is completely determined by its two-point

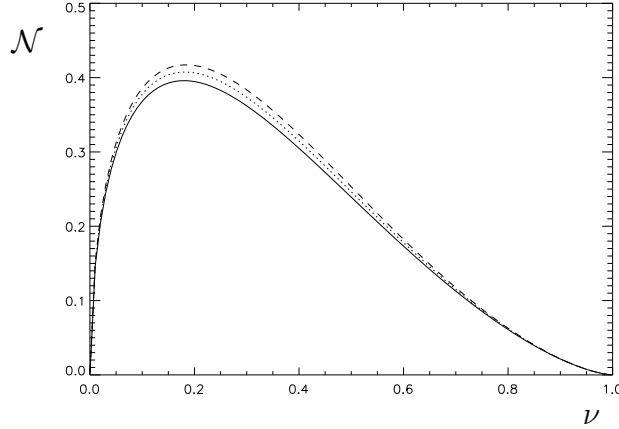


Figure 2: Function  $\mathcal{N}(a, \nu)$  at  $a = 1$  for different values of the equation of state parameter of phantom energy,  $w_p = -1.0$ ,  $w_p = -1.17$  and  $w_p = -1.33$  (solid, dotted and dashed lines, respectively).

correlation function, which we parametrize as follows,

$$\langle A(\mathbf{k})A^*(\mathbf{k}') \rangle = \frac{f(k)}{k^3} \frac{M^2}{M_{PL}^2} \delta(\mathbf{k} - \mathbf{k}'). \quad (9)$$

Let us clarify the form chosen for the overall factor. We begin with the factor  $M_{PL}^{-2}$ . Let us recall that the gravitational potential is generated by the perturbations of the phantom field, which in turn is assumed to cause the accelerated cosmological expansion. This implies, in particular, that the energy density of the homogeneous phantom field is of the order of the present critical density,

$$\rho_p \sim M_{PL}^2 H_0^2. \quad (10)$$

On the other hand, this energy density can be estimated as

$$\rho_p \sim M_X^2 X^2, \quad (11)$$

where  $M_X$  is the mass scale characteristic of the phantom field and  $X$  estimates the value of this field. By comparing eq. (10) to eq. (11) we obtain an estimate for this value,

$$X \sim \frac{M_{PL} H_0}{M_X}.$$

Let us assume that all dimensionful parameters in the phantom Lagrangian are of order of the mass parameter  $M$  entering the dispersion relation (1), so that  $M_X \sim M$ . We estimate the amplitude of vacuum fluctuations of physical momenta of order  $M$  as  $\delta X \sim M$ . Therefore,

$$\delta \rho_p \sim M_X^2 X \delta X \sim M^2 M_{PL} H_0.$$



Now, we make use of the Poisson equation for the gravitational potential,

$$\Delta\Phi \sim \frac{\delta\rho_p}{M_{PL}^2},$$

and find that at physical momenta of order  $M$  the gravitational potential is of order

$$\Phi \sim \frac{H_0}{M_{PL}}.$$

This gives rise to the factor  $M_{PL}^{-2}$  in (9). The factor  $M^2$  is introduced on dimensional grounds. The dimensionless function  $f(k)$  in (9) parametrizes possible deviations from the flat spectrum; it is likely that this function is model-dependent. However, we have seen that the growth factor  $\exp[N(a, \nu)]$  is peaked at  $\nu = \nu_{max}$ . This implies that the integrals over conformal momenta, determining CMB anisotropies, are saturated in a narrow region of  $k$ . Hence, if  $f(k)$  is sufficiently smooth, our final results are insensitive to its shape, so we can set  $f(k) = C$  where  $C$  is a constant. This constant may be somewhat different from 1, as it may contain, e.g., a power of  $H_0/M$ ; it cannot, however, contain extra factors involving the Planck mass. We will see that our final results are determined by the interplay between the large growth factor  $\exp(N)$  and small factor  $\propto M_{PL}^{-1}$  in  $A(\mathbf{k})$ , so a possible deviation of  $C$  from unity is unimportant in the end. Furthermore, we will see that the shape of the tachyonic contribution to the CMB anisotropy spectrum (the position of the maximum and width) is independent of  $M$ ; the parameter  $M$  determines the overall magnitude only. Therefore, the constant  $C$  can be set equal to 1 by redefinition of the parameter  $M$ . In view of these observations we write for the two-point correlator, without loss of generality,

$$\langle A(\mathbf{k})A^*(\mathbf{k}') \rangle = \frac{M^2}{M_{PL}^2} \frac{1}{k^3} \delta(\mathbf{k} - \mathbf{k}') . \quad (12)$$

It is this expression that will be used in what follows. Note that the amplitude  $A(\mathbf{k})$  is very small, so the linearized treatment of the problem is legitimate even for exponentially growing gravitational potential.

### 3.2 Lorentz-invariant model.

The analysis performed in section 3.1 is straightforwardly repeated in the case of Lorentz-invariant dispersion relation (2). There are two properties, however, that make this case different from the Lorentz-violating one. The first property has to do with the behaviour of the function  $\mathcal{N}(a, \nu)$  that enters the growth factor,

$$N(a, \nu) = \frac{M}{H_0} \mathcal{N}(a, \nu) . \quad (13)$$

In the Lorentz-invariant case one has

$$\mathcal{N}(a, \nu) = \int_{\nu}^a d\hat{a} \frac{\sqrt{\hat{a}^2 - \nu^2}}{\sqrt{\hat{a}} \sqrt{\Omega_m + \Omega_p \hat{a}^{-3w_p}}} . \quad (14)$$

Unlike in the Lorentz-violating model,  $\mathcal{N}(a, \nu)$  as a function of  $\nu$  monotonously decreases as  $\nu$  increases, so the maximum of  $\mathcal{N}(a, \nu)$  is at  $\nu = 0$ . It is therefore instructive to find  $\mathcal{N}(a, \nu)$  at small  $\nu$ . To this end, we write for the integral (14)

$$\mathcal{N} = \mathcal{N}_0 + \mathcal{N}_1 + \mathcal{N}_2,$$

where

$$\mathcal{N}_0 = \int_{\nu}^a d\hat{a} \frac{\hat{a}}{\sqrt{\hat{a}} \sqrt{\Omega_m + \Omega_p \hat{a}^{-3w_p}}}, \quad (15)$$

$$\mathcal{N}_1 = \int_{\nu}^{\infty} d\hat{a} \frac{\sqrt{\hat{a}^2 - \nu^2} - \hat{a}}{\sqrt{\hat{a}} \sqrt{\Omega_m + \Omega_p \hat{a}^{-3w_p}}}, \quad (16)$$

$$\mathcal{N}_2 = - \int_a^{\infty} d\hat{a} \frac{\sqrt{\hat{a}^2 - \nu^2} - \hat{a}}{\sqrt{\hat{a}} \sqrt{\Omega_m + \Omega_p \hat{a}^{-3w_p}}}. \quad (17)$$

The integrals (16), (17) are convergent, since at large  $\hat{a}$  one has

$$\sqrt{\hat{a}^2 - \nu^2} - \hat{a} \simeq -\frac{\nu^2}{2\hat{a}}.$$

Furthermore, the latter expression shows that at small  $\nu$  the integral (17) is of order  $\nu^2$ . The integral (16) can be written as

$$\mathcal{N}_1 = \nu^{3/2} \int_1^{\infty} dy \frac{\sqrt{y^2 - 1} - y}{\sqrt{y} \sqrt{\Omega_m + \Omega_p \nu^{-3w_p} y^{-3w_p}}}.$$

Since  $w_p < 0$ , the term with  $\Omega_p$  in the integrand can be neglected at small  $\nu$ , and then the remaining integral is straightforwardly evaluated. Finally, the integral  $\mathcal{N}_0$  is readily calculated at<sup>3</sup>  $w_p = -1$ ,

$$\begin{aligned} \mathcal{N}_0 &= \int_{\nu}^a d\hat{a} \frac{\sqrt{\hat{a}}}{\sqrt{\Omega_m + \Omega_p \hat{a}^3}} = \frac{2}{3\sqrt{\Omega_p}} \left( \text{Arcsinh} \sqrt{a^3 \frac{\Omega_p}{\Omega_m}} - \text{Arcsinh} \sqrt{\nu^3 \frac{\Omega_p}{\Omega_m}} \right) \\ &= \frac{2}{3\sqrt{\Omega_p}} \text{Arcsinh} \sqrt{a^3 \frac{\Omega_p}{\Omega_m}} - \frac{2}{3\sqrt{\Omega_m}} \nu^{3/2} + \mathcal{O}(\nu^{9/2}). \end{aligned}$$

---

<sup>3</sup>Like in the Lorentz-violating case, the dependence on  $w_p$  is weak.

With all contributions included, we obtain finally that at small  $\nu$

$$\mathcal{N}(a, \nu) = \frac{2}{3\sqrt{\Omega_p}} \text{Arcsinh} \sqrt{a^3 \frac{\Omega_p}{\Omega_m}} - \frac{\mathcal{C}}{\sqrt{\Omega_m}} \nu^{3/2} + \mathcal{O}(\nu^2), \quad (18)$$

$$\mathcal{C} = \frac{2}{3} - \int_1^\infty dy \frac{\sqrt{y^2 - 1} - y}{\sqrt{y}} = \sqrt{\pi} \frac{\Gamma(-3/4)}{\Gamma(-1/4)} \simeq 1.75. \quad (19)$$

Note that the expressions (13) and (18) imply that the tachyonic contribution is not negligible only for  $M > H_0$ . This is the analog of the inequality (8).

It is clear from eq. (18) that unlike in the Lorentz-violating case, the growth factor  $\exp[N(a, \nu)]$  is peaked at  $\nu = 0$ . This is due to the fact that low-momentum modes are tachyonic already at early times, and their “frequency”  $\omega = M$  is not small. However, the modes of very low spatial momenta  $k = M\nu$  contribute to the *monopole* CMB harmonic only. This contribution strongly depends on the primordial spectrum of the tachyonic perturbations, i.e., on the shape of the function  $f(k)$  in (9); this is the second special property of the Lorentz-invariant model. Now, the monopole contribution merely renormalizes the average CMB temperature; it is not directly measurable and will not be discussed in this paper. Multipoles with  $l \neq 0$  are less model-dependent: we will see in section 4.2 that the integrals over momenta are saturated in a relatively narrow region where  $N(a, \nu)$  is not damped, i.e., in the region where

$$\nu \sim \left( \frac{H_0}{M} \right)^{2/3}. \quad (20)$$

We assume that  $f(k)$  does not change much in an interval  $\Delta k \sim k$  for momenta belonging to the region (20). Then for calculating the CMB multipoles with  $l \neq 0$ , we can still use the spectrum (12).

## 4 CMB multipoles

The contribution to CMB anisotropy we are interested in is generated fairly recently, when the tachyon-induced gravitational potential becomes sizeable. Therefore, the only phenomenon responsible for this contribution is the integrated Sachs–Wolfe effect. It is clear from Fig. 1 that in the Lorentz-violating model this effect operates at the late cosmological epoch beginning at  $z \sim 0.05$  ( $a \sim 0.95$ ). Similar picture holds in the Lorentz-invariant case.

Let us use the standard notation for the temperature anisotropy

$$\Theta(\mathbf{n}) = \frac{T(\mathbf{n}) - T_0}{T_0},$$

where  $\mathbf{n}$  is the direction of observation and  $T_0$  is the average CMB temperature at present. The integrated Sachs–Wolfe effect then reads (see, e.g., Ref. [19])

$$\Theta(\mathbf{n}) = 2 \int_0^{\eta_0} d\eta \left. \frac{\partial \Phi(\eta, \mathbf{x})}{\partial \eta} \right|_{\mathbf{x}=\mathbf{n}(\eta_0-\eta)}, \quad (21)$$

where  $\eta_0$  is the present time, and in view of the above discussion we set the lower limit of integration equal to zero instead of the time of last scattering. The integrand in (21) exponentially grows towards the present epoch.

CMB anisotropy is characterized by the multipoles

$$C_l = \frac{1}{2l+1} \sum_{m=-l}^{m=l} \langle |a_{lm}|^2 \rangle, \quad (22)$$

where  $a_{lm}$  are the coefficients of the decomposition of the anisotropy over spherical harmonics,

$$a_{lm} = \int d\mathbf{n} \Theta(\mathbf{n}) Y_{lm}(\mathbf{n}). \quad (23)$$

Making use of eqs. (3), (12) and (21) and performing the angular integration one obtains the following expression for the multipoles in terms of integrals over conformal momenta,

$$C_l = \frac{8M^2}{\pi M_{PL}^2} \int_0^1 \frac{d\nu}{\nu} \Delta_l^2(\nu) \quad (24)$$

The quantity  $\Delta_l^2(\nu)$  is the analog of power spectrum. It is expressed in terms of the integral over conformal time,

$$\Delta_l(\nu) = \int_{\eta_k}^{\eta_0} d\tau \omega(\tau) a(\tau) \exp \{N[a(\tau), \nu]\} j_l[M\nu(\eta_0 - \tau)], \quad (25)$$

where

$$j_l(x) = \sqrt{\frac{\pi}{2x}} J_{l+\frac{1}{2}}(x)$$

is the spherical Bessel function of the first kind. The integrals (25) and (24) have different properties in Lorentz-violating and Lorentz-invariant models.

## 4.1 Lorentz-violating model.

We plot in the left panel of Fig. 3 the tachyonic contribution to the angular spectrum of CMB temperature in the Lorentz-violating model with  $\alpha = 1 \cdot 10^{-3}$  and  $M/H_0 = 9770$ , using the standard quantity

$$D_l = \frac{l(l+1)}{2\pi} C_l,$$

It is clear that the spectrum has rather narrow maximum at  $l = l_{\max}$  ( $l_{\max} \approx 7$  in the example shown in Fig. 3). We will see below that the position of the maximum is determined solely by the parameter  $\alpha$ , and that  $l_{\max}$  grows as  $\alpha$  decreases, see eq. (33).

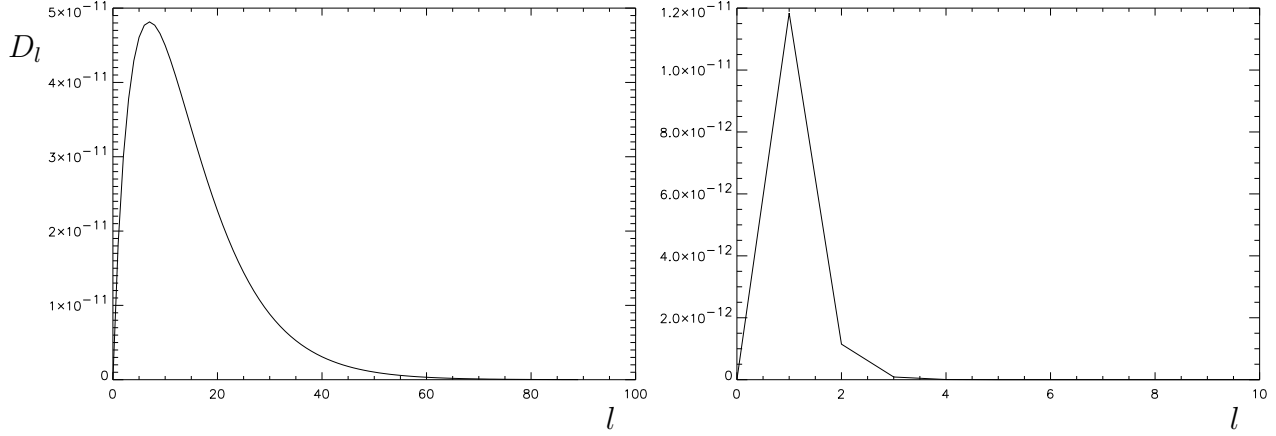


Figure 3: **Left:** The tachyonic contribution to the angular spectrum of CMB temperature in the Lorentz-violating model with  $\alpha = 1 \cdot 10^{-3}$  and  $M/H_0 = 9770$ . **Right:** Same, but for  $\alpha = 1.0$  and  $M/H_0 = 315$ .

For  $\alpha = 1$ , the spectrum is shown in the right panel of Fig. 3. It is clear from this figure that at large enough  $\alpha$ , the tachyonic perturbations contribute to the lowest multipoles only. It is also clear that the dipole and quadrupole components differ by one order of magnitude only. Hence, we disregard in what follows the dipole component, as for realistic quadrupole it is negligible compared to the observed dipole which is supposedly due to the motion of the Earth in the CMB reference frame. We note in passing that the situation is different in the Lorentz-invariant model: it is meaningful to discuss the dipole component in that case, see sections 4.2 and 5.2.

The multipoles  $C_l$  can be calculated analytically in the regime  $\alpha(M/H_0)^2 \gg 1$ , see (8). As we discussed in section 3.1, the function  $\exp[N(a, \nu)]$  rapidly grows with the scale factor, and as a function of  $\nu$  it has a peak at  $\nu_{\max} \simeq 0.2$ . Thus, the main contribution into the integral (25) comes from late times, while the integral (24) is saturated at  $\nu \approx \nu_{\max}$  (it is important at this point that  $\nu_{\max}$  is different from both 0 and 1). This means, in the first place, that the lower limit of integration in (25) may be set equal to zero. Second, one can make use of expansion of the function  $N(a, \nu)$  near  $a = 1$ ,

$$N[a(\eta), \nu] = N(1, \nu) - \omega(\nu) \cdot (\eta_0 - \eta), \quad (26)$$

and for  $\nu = \nu_{\max} \simeq 0.2$  we have

$$N(1, \nu_{\max}) = 0.39\sqrt{\alpha}\frac{M}{H_0}.$$

Third, one can set the pre-exponential factor  $\omega(\eta)a(\eta)$  in (25) equal to its value at  $a = 1$ . In this way we obtain

$$\Delta_l(\nu) = \sqrt{\alpha} \sqrt{\frac{1-\nu}{\nu}} \exp[N(1, \nu)] \int_0^{\nu M \eta_0} dx \exp\left(-\sqrt{\alpha} \sqrt{\frac{1-\nu}{\nu}} x\right) j_l(x), \quad (27)$$

where we introduced the integration variable  $x = \nu M(\eta_0 - \eta)$ . Finally, let us recall that  $\eta_0 \sim 1/H_0$ . Then the upper limit of integration in (27) is  $\nu M \eta_0 \sim \nu_{\max} M/H_0 \gg 1$ , so the integration may be extended to infinity. Then the integral in (27) is calculated by making use of the formula [20]

$$\begin{aligned} \int_0^\infty dx \frac{J_{l+\frac{1}{2}}(x)}{\sqrt{x}} \exp(-\gamma x) &= \frac{1}{(1+\gamma^2)^{\frac{1}{4}}} \Gamma(l+1) P_{-\frac{1}{2}}^{-l-\frac{1}{2}} \left[ \frac{\gamma}{\sqrt{1+\gamma^2}} \right] = \\ &= \frac{1}{(1+\gamma^2)^{\frac{1}{4}}} \frac{\Gamma(l+1)}{\Gamma(l+\frac{3}{2})} \left[ \frac{1-z}{1+z} \right]^{\frac{l}{2}+\frac{1}{4}} F\left(\frac{1}{2}, \frac{1}{2}, l+\frac{3}{2}, \frac{1-z}{2}\right), \end{aligned} \quad (28)$$

where  $P_{-\frac{1}{2}}^{-l-\frac{1}{2}}$  is the Legendre function,  $F$  is the hypergeometric function<sup>4</sup>, and

$$z = \frac{\gamma}{\sqrt{1+\gamma^2}} = \sqrt{\frac{\alpha(1-\nu)}{\nu + \alpha(1-\nu)}}.$$

Due to the exponential dependence on  $\nu$  of the factor  $\exp[N(1, \nu)]$  in (27), the integral in (24) can be evaluated in the saddle-point approximation, and we obtain

$$\begin{aligned} D_l &= \frac{2M^2}{M_{PL}^2 \nu_{\max}} \sqrt{\frac{1}{\pi |N''(1, \nu_{\max})|}} \exp(2N(1, \nu_{\max})) \cdot l(l+1) \cdot \left[ \frac{\Gamma(l+1)}{\Gamma(l+3/2)} \right]^2 \times \\ &\times \frac{z^2}{\sqrt{1-z^2}} \left( \frac{1-z}{1+z} \right)^{l+1/2} F^2\left(\frac{1}{2}, \frac{1}{2}, l+\frac{3}{2}, \frac{1-z}{2}\right), \end{aligned} \quad (29)$$

where  $z = z(\nu_{\max})$ ,  $N''(1, \nu)$  is the second derivative with respect to  $\nu$ . At  $\nu_{\max} \simeq 0.2$  we have

$$D_l = \mathcal{A}_0 \cdot \left[ \frac{\Gamma(l+1)}{\Gamma(l+3/2)} \right]^2 \frac{l(l+1)}{\sqrt{1+4\alpha}} \cdot \left( \frac{1-z}{1+z} \right)^{l+1/2} F^2\left(\frac{1}{2}, \frac{1}{2}; l+\frac{3}{2}, \frac{1-z}{2}\right), \quad (30)$$

$$z = \frac{2\sqrt{\alpha}}{\sqrt{1+4\alpha}},$$

$$\mathcal{A}_0 = 9.4 \cdot \left( \sqrt{\alpha} \frac{M}{H_0} \right)^{3/2} \left( \frac{H_0}{M_{PL}} \right)^2 \cdot \exp \left[ 0.78 \sqrt{\alpha} \frac{M}{H_0} \right]. \quad (31)$$

---

<sup>4</sup>The second representation of the integral (28) is convenient because the hypergeometric function is only slightly different from unity at  $0 \leq z \leq 1$ , which corresponds to  $0 \leq \alpha < \infty$ .

This is the desired analytical expression for the multipoles; it works with the precision which is certainly sufficient for our purposes..

At  $\alpha \ll 1$  and  $l > 1$ , the expression (29) simplifies to

$$D_l = \frac{2\alpha M^2}{M_{PL}^2} \frac{1 - \nu_{\max}}{\nu_{\max}^2} \sqrt{\frac{1}{\pi |N''(1, \nu_{\max})|}} \exp(2N(1, \nu_{\max})) \cdot (l + 1) \cdot \exp\left(-2l\sqrt{\alpha} \sqrt{\frac{1 - \nu_{\max}}{\nu_{\max}}}\right). \quad (32)$$

Corrections to the latter formula are  $\mathcal{O}(1/l)$  and they are numerically small even for  $l = 2$ .

A few comments are in order. First, it is seen from (30) that the dependence on  $l$  and on  $M$  has factorized. Therefore, the position of the maximum  $l_{\max}$  and the width of the peak in the spectrum depend on the parameter  $\alpha$  and do not depend on the parameter  $M$ . In particular, for  $\alpha \ll 1$  the maximum of the function (32) is at

$$l_{\max} = \frac{1}{2\sqrt{\alpha}} \sqrt{\frac{\nu_{\max}}{1 - \nu_{\max}}} - 1 \simeq \frac{1}{4\sqrt{\alpha}} - 1. \quad (33)$$

The overall magnitude of the spectrum depends on both  $\alpha$  and  $M$ . The dependence on  $M$  is exponential, since  $N(1, \nu_{\max}) \propto M$ . This justifies the use of (12) for the primordial spectrum of perturbations of the gravitational potential.

Second, the exponential dependence of  $C_l$  on  $l$  has the following interpretation. The problem has the characteristic time scale  $\tau(k) \sim \omega^{-1} = (\sqrt{\alpha} M \sqrt{\nu(1 - \nu)})^{-1} \ll H_0^{-1}$ . This scale determines the time of the development of the tachyonic instability in a mode with momentum  $k$ . Since the growth function  $N(\nu)$  has a maximum, the relevant modes have momenta near  $k_{\max} = \nu_{\max} M$ . Therefore, the gravitational potential is small at distances  $r \gg \tau(k_{\max})$  along the light cone emanating from the observer (the tachyonic instability has not developed yet). On the other hand, at distances  $r < \tau(k_{\max})$  the gravitational potential is almost constant in time (according to (8), the expansion of the Universe makes negligible effect, while the tachyonic instability gives rise to mild growth of the potential). In other words, the gravitational potential at  $r < \tau(k_{\max})$  is the superposition of random, time-independent waves with almost constant amplitude and almost constant wavelength  $2\pi/k_{\max}$ . At  $r > \tau(k_{\max})$  the amplitude of these waves decays as  $\exp[-r/\tau(k_{\max})]$  as  $r$  increases. The period of a wave located at distance  $r$  is seen at an angle  $\Delta\theta_r \simeq 2\pi/(rk_{\max})$ . Hence, this wave contributes to the multipoles with  $l \simeq rk_{\max}$ . The multipoles  $a_{lm}$  are not exponentially suppressed for  $r < \tau(k_{\max})$ , i.e.,  $l < 1/[k_{\max}\tau(k_{\max})]$ , and are exponentially small in the opposite case. Recalling (22), one finds that this behaviour of  $a_{lm}$  leads to the following dependence of  $C_l$  on  $l$ ,

$$C_l \propto \exp\left(-\frac{2l}{k_{\max}\tau(k_{\max})}\right) = \exp\left(-2l\sqrt{\alpha} \sqrt{\frac{1 - \nu_{\max}}{\nu_{\max}}}\right),$$

in complete agreement with (33).

The fact that for relatively large  $\alpha$  sizeable contributions are obtained by the lowest multipoles only (see Fig. 3) is seen directly from (21). Indeed, inserting (3) into (21), making use of (26), and integrating over time, we obtain

$$\Theta(\mathbf{n}) \sim \int d^3k F(k, \omega) A(\mathbf{k}) \frac{1}{\sqrt{\alpha} \sqrt{\frac{1-\nu}{\nu}} - i \frac{\mathbf{k} \cdot \mathbf{n}}{k}} + \text{h.c.}, \quad (34)$$

where  $F(k, \omega)$  is a smooth function independent of the direction of  $\mathbf{k}$ . Recalling that  $\nu \simeq \nu_{\max} = 0.2$ , we have  $\sqrt{\alpha} \sqrt{(1-\nu)/\nu} > 1$  for sufficiently large  $\alpha$ . In that case the denominator in (34) can be expanded in a series in  $(\mathbf{k} \cdot \mathbf{n})$ , which just corresponds to the expansion in spherical harmonics. The  $l$ -th harmonic is thus suppressed as  $(\sqrt{\alpha} \sqrt{(1-\nu)/\nu})^{-l}$ . This is relatively mild suppression, in accord with the right panel of Fig. 3. At  $\sqrt{\alpha} \sqrt{(1-\nu)/\nu} < 1$  the expansion of the denominator in (34) is not legitimate, and one has to perform more sophisticated analysis leading to (30).

## 4.2 Lorentz-invariant model.

In the Lorentz-invariant case we make use of the expression (18) for the function  $\mathcal{N}(a, \nu)$  to calculate the integral (25). We find

$$\Delta_l(\nu) = \frac{\sqrt{\pi}}{2} \frac{\Gamma(l+1)}{\Gamma(l+3/2)} \left(\frac{\nu}{2}\right)^l \cdot \exp \left( \frac{2}{3} \frac{M}{H_0 \sqrt{\Omega_p}} \text{Arcsinh} \sqrt{\frac{\Omega_p}{\Omega_m}} - \frac{\mathcal{C}M}{H_0 \sqrt{\Omega_m}} \nu^{3/2} \right). \quad (35)$$

When obtaining this expression we used the fact that  $\nu$  is small (see (20)), again extended the time integration to infinity in the same way as we have done after eq. (27) and made use of eq. (28). We also kept the leading terms in  $\nu$  in the expression (35).

Inserting (35) into the expression (24) for multipoles, and changing the integration variable, we arrive at the following integral

$$\left( \frac{H_0 \sqrt{\Omega_m}}{2\mathcal{C}M} \right)^{4l/3} \int_0^{\frac{\mathcal{C}M}{H_0 \sqrt{\Omega_m}}} dx x^{4l/3-1} e^{-x} = \left( \frac{H_0 \sqrt{\Omega_m}}{\mathcal{C}M} \right)^{4l/3} \gamma \left( \frac{4l}{3}, \frac{\mathcal{C}M}{H_0 \sqrt{\Omega_m}} \right), \quad (36)$$

where  $\gamma(\beta, x)$  is incomplete  $\Gamma$ -function. We notice that the second argument of this function,

$$x = \frac{\mathcal{C}M}{H_0 \sqrt{\Omega_m}},$$

is large,  $x \gg 1$ , otherwise the overall factor in (24) makes the effect we discuss negligibly small. Hence, for  $\beta \equiv 4l/3 \ll x$  we use the approximation  $\gamma(\beta, x) = \Gamma(\beta)$ , and obtain the



final formula for the multipoles,

$$D_l = \frac{M^2}{3\pi M_{PL}^2} \frac{l(l+1)}{2^{2l-1}} \exp\left(\frac{4M}{3H_0} \frac{1}{\sqrt{\Omega_p}} \text{Arcsinh}\sqrt{\frac{\Omega_p}{\Omega_m}}\right) \left[\frac{\Gamma(l+1)}{\Gamma(l+3/2)}\right]^2 \left(\frac{H_0\sqrt{\Omega_m}}{2\mathcal{C}M}\right)^{\frac{4l}{3}} \Gamma\left(\frac{4l}{3}\right). \quad (37)$$

This formula is valid for relatively low multipoles,  $l < \mathcal{C}M/(H_0\sqrt{\Omega_m})$ . In the opposite case the behaviour of the incomplete  $\Gamma$  function is

$$\gamma(\beta, x) \simeq \frac{x^\beta}{\beta} e^{-x}$$

Hence, the multipoles at large  $l$  are negligibly small in the interesting case of large  $x$ .

Due to the exponential factor in (37), the low multipoles may be fairly large at large enough  $M/H_0$ . On the other hand, large value of this parameter implies that the multipoles rapidly decay with  $l$ ; as we discuss in section 5.2, the interesting range is  $M/H_0 \sim 100$ , in which case the multipole  $D_{l+1}$  is suppressed by a factor of about  $10^{-3}$  as compared to  $D_l$ . So, it is sufficient to consider the dipole and quadrupole anisotropies only. With our parametrization, these are, respectively,

$$D_1 = 6.4 \cdot 10^{-125} \left(\frac{M}{H_0}\right)^{2/3} \exp\left(1.98 \cdot \frac{M}{H_0}\right) \quad (38)$$

$$D_2 = 4.1 \cdot 10^{-126} \left(\frac{H_0}{M}\right)^{2/3} \exp\left(1.98 \cdot \frac{M}{H_0}\right) \quad (39)$$

$$\frac{D_1}{D_2} = 15.7 \left(\frac{M}{H_0}\right)^{4/3} \quad (40)$$

These expressions are in agreement, within 10%, with the values that we obtained numerically<sup>5</sup>.

## 5 Comparison with the data

Overall, the data on the anisotropy of CMB temperature are in good agreement with the standard picture of adiabatic scalar perturbations whose primordial spectrum is close to the Harrison–Zeldovich one. Still, the observed angular spectrum may possibly show deviations whose nature is unclear. Our analysis was partially motivated by the desire to understand whether these deviations may be due to the contributions coming from the tachyonic perturbations of phantom energy. As we discuss in this section, the deviations *cannot* be explained in this way. So, our analysis enables us only to place limits on the parameters of the tachyonic perturbations.

---

<sup>5</sup>The reason for the 10% discrepancy is the omission of the term of order  $\nu^2$  in the expression (18) for  $\mathcal{N}(a, \nu)$ ; note that  $\mathcal{N}(a, \nu)$  enters the final result exponentially.

## 5.1 Lorentz-violating case.

We begin with the Lorentz-violating model, and consider a wide range of the parameter  $\alpha$ ,

$$2.5 \cdot 10^{-7} < \alpha < 1.0. \quad (41)$$

This range is representative: at  $\alpha \gtrsim 1$  the main effect is in the lowest multipoles, whereas at  $\alpha = 2.5 \cdot 10^{-7}$  the contribution is peaked at  $l \sim l_{\max} \simeq 500$ , see (33). As we pointed out above, we do not consider the dipole anisotropy in the Lorentz-violating case, as it is much smaller than the observed dipole anisotropy supposedly originating from the motion of the Earth.

In our study we used the data on multipoles given in Ref. [21] and organized as a table “ $C_l$  vs.  $l$ ”. These are not combined in bins, unlike the data usually presented.

In the model we study, the

multipoles are the sums of two terms, one due to adiabatic scalar perturbations and another due to tachyonic modes,

$$C_l = C_l^{(ad)} + C_l^{(t)}. \quad (42)$$

Making use of the code CMBFast [22], we calculated the angular spectrum  $C_l^{(ad)}$  generated by adiabatic scalar perturbations for various values of the spectral index  $n_s$  in the range  $0.8 \leq n_s \leq 1.5$ , in the standard cosmological model with the following values of parameters: the Hubble constant  $H_0 = 72 \text{ km} \cdot \text{s}^{-1} \cdot \text{Mpc}^{-1}$ , baryon plus CDM contribution to the present energy density  $\Omega_m = 0.27$ , contribution of hot dark matter  $\Omega_{hdm} = 0$ , dark energy contribution  $\Omega_p \equiv \Omega_\Lambda = 0.73$ ,  $^4\text{He}$  abundance  $Y = 0.24$ , number of massless neutrino species  $N_\nu = 3$ . We assumed that the tensor perturbations are absent. The second term  $C_l^{(t)}$  in (42) was calculated by making use of the analytical expression (30).

To compare the model with the data, we analyzed the difference between the measured and calculated multipoles,

$$\epsilon_l = C_l^{(exp)} - C_l^{(ad)} - C_l^{(t)}.$$

The study of the moments and correlation properties of  $\epsilon_l$  has shown that they are independent and their average is zero within statistical error. Furthermore,  $\chi^2$  estimate has shown that with 95% probability the distribution of  $\epsilon_l$  is Gaussian.

To obtain the parameters of the theoretical spectrum, we used maximum likelihood method with the likelihood function

$$\begin{aligned} F(\epsilon|\theta) &= \prod_{l=2,600} f(\epsilon_l|\theta), \\ f(\epsilon_l|\theta) &= \exp\left(-\frac{\epsilon_l^2(\theta)}{2\sigma_l^2}\right). \end{aligned}$$

Here  $\theta$  is the set of four parameters: the spectral index and amplitude of adiabatic perturbations, the amplitude  $\mathcal{A}_0$  and parameter  $\alpha$  of the tachyonic perturbations. In view of (33) and (41), we included in our analysis multipoles with  $l \leq 600$  only. For each  $\alpha$  from the range (41) we obtained the best fit values of the three other parameters. The variations of individual multipoles have been calculated with the use of the error estimations given in the third column of the table in Ref. [21].

We show in Fig. 4 the best fit value of the tachyonic contribution as a function of the parameter  $\alpha$ . As a measure of this contribution we use the maximum in the anisotropy spectrum generated by the tachyonic perturbations,

$$D_{\max} = \max_l \left[ \frac{l(l+1)}{2\pi} C_l^{(t)} \right]. \quad (43)$$

This maximum is at  $l = l_{\max}$  (as an example,  $l_{\max} \approx 7$  in the left panel of Fig. 3). It is clear from Fig. 4 that at  $\alpha > 10^{-4}$  the best fit value is equal to zero, whereas at  $\alpha < 10^{-4}$  it is considerably different from zero. This means that the tachyonic contribution improves the agreement between the theory and data. It is worth noting that the addition of this contribution moves the best fit value of the spectral index up from  $n_s = 0.96$  obtained in Ref. [23]; in particular, for some values of  $\alpha$  the best fit values of  $n_s$  are larger than 1.

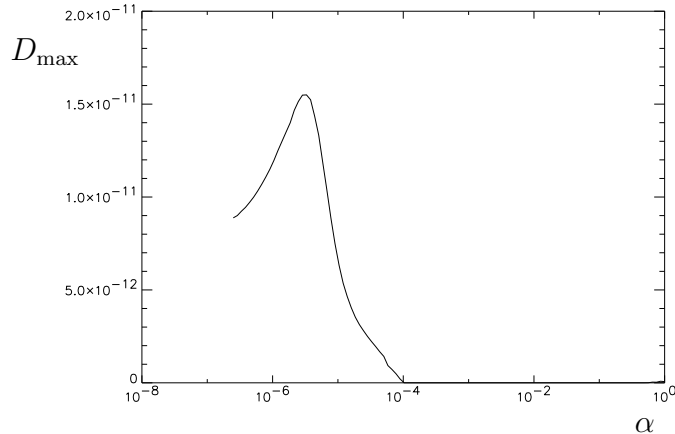


Figure 4: The best fit value of the tachyonic contribution to CDM temperature anisotropy as a function of  $\alpha$ . The parameter  $D_{\max}$  is defined in (43). The maximum of  $D_{\max}$  is at  $\alpha = 3.0 \cdot 10^{-6}$ , which corresponds to  $l_{\max} \simeq 143$ .

This improvement, however, is not statistically significant. We show in Fig. 5 the maximum likelihood function as a function of  $D_{\max}$  at  $\alpha = 1.8 \cdot 10^{-6}$ . It is clear from Fig. 5, that even though the best fit value of  $D_{\max}$  is non-zero, the difference of the likelihood function at the best fit value and at  $D_{\max} = 0$  is small. The same is true for all values of  $\alpha$  in the

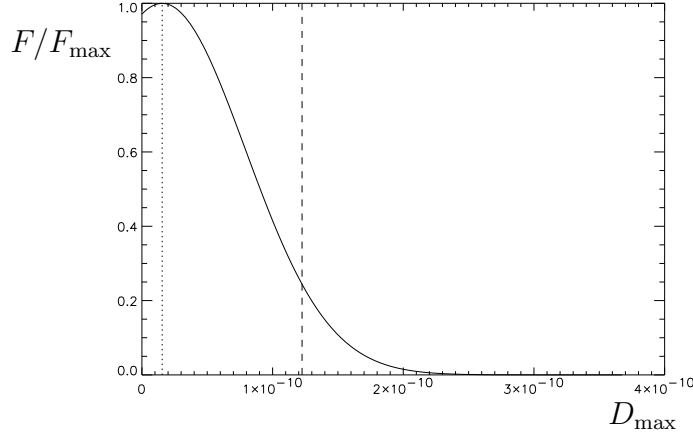


Figure 5: Likelihood function at the best fit values of the amplitude and spectral index of the adiabatic perturbations as a function of  $D_{\text{max}}$  at  $\alpha = 1.8 \cdot 10^{-6}$ . The dashed line shows the limit on  $D_{\text{max}}$  at 95 % confidence level. Dotted line corresponds to the best fit value of  $D_{\text{max}}$ . The maximum value of the likelihood function is  $F_{\text{max}} = 0.577$ .

range considered. So, the data is consistent with the absence of the tachyonic contribution to the CMB temperature anisotropy.

Thus, we can only place limits on the overall magnitude of the tachyonic contribution,  $\mathcal{A}_0$ , at various values of  $\alpha$ , which can then be translated into the limits on the physical parameter  $M/H_0$ . These limits, at 95 % confidence level, are shown in Fig. 6.

## 5.2 Lorentz-invariant case.

As we have seen in section 4.2, in the model with Lorentz-invariant spectrum the CMB multipoles generated by the tachyonic perturbations rapidly decrease as  $l$  increases. Therefore, only two multipoles — the dipole and quadrupole — are relevant for comparison with the data. The measured dipole component of CMB temperature is [24]  $d = 3.358 \pm 0.017$  mK, and the direction in the Galactic polar coordinate frame is  $l = 263.86 \pm 0.04^\circ$ ,  $b = 48.24 \pm 0.10^\circ$ . In the standard parametrization, the dipole anisotropy is

$$D_1^{\text{exp}} = \frac{1}{3\pi} \sum_{m=-1}^{m=1} |a_{1m}|^2 = 1.6 \cdot 10^{-7}, \quad (44)$$

while the quadrupole component is given by

$$D_2^{\text{exp}} = \frac{3}{5\pi} \sum_{m=-2}^{m=2} |a_{2m}|^2 = 2.9 \cdot 10^{-11}. \quad (45)$$

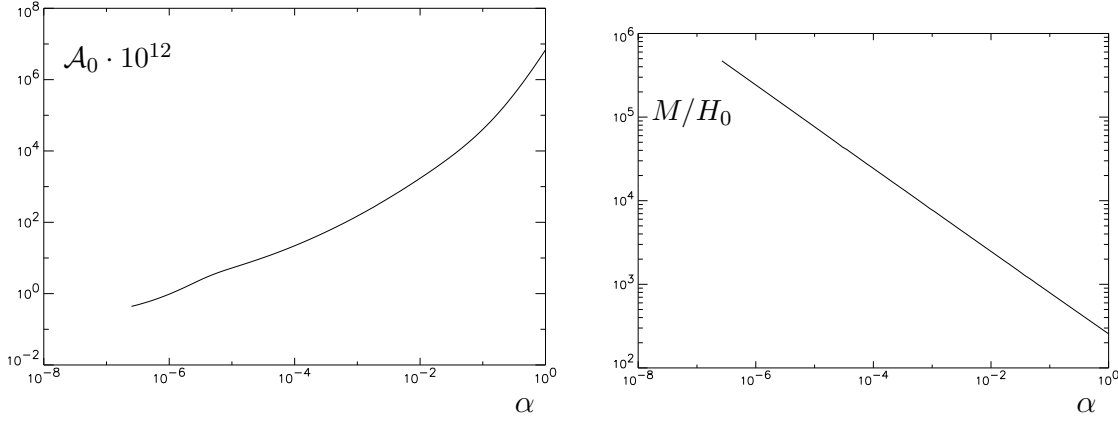


Figure 6: **Left:** upper limit on the amplitude  $\mathcal{A}_0$  for  $\alpha \in [1.0 \div 2.5 \cdot 10^{-7}]$  at 95 % confidence level. **Right:** upper limit on the parameter  $M$  of the tachyonic perturbations in units of the Hubble constant, at 95 % confidence level.

To obtain conservative limits on the parameter  $M$  of Lorentz-invariant tachyonic perturbations, we do not impose any priors on the contribution to the dipole anisotropy due to the motion of the Earth and on the quadrupole anisotropy generated by adiabatic perturbations. We make use of the expression (38) and take into account the fact that the dipole has 3 degrees of freedom. In this way we find that the analysis of the dipole anisotropy leads to the limit

$$\frac{M}{H_0} \leq 135.9 \quad \text{at 95 \% c.l.} \quad (46)$$

The limit coming from the quadrupole anisotropy is obtained by making use of eq. (39). It reads

$$\frac{M}{H_0} \leq 136.4 \quad \text{at 95 \% c.l.} \quad (47)$$

Interestingly, the limit coming from the dipole anisotropy is similar to that obtained from the quadrupole. One can turn this result around and speculate that the large observed dipole may be due to the tachyonic perturbations, with no contradiction to the data at higher multipoles. In our model the latter property is natural in the sense that the quadrupole and higher angular harmonics are small automatically. Another way to phrase this is to pretend that the observed dipole anisotropy is due to the tachyonic perturbations, i.e., equate (38) and (44), and then calculate the contribution to the quadrupole from (39). This gives for the tachyonic contribution  $D_2 = 1.5 \cdot 10^{-11}$ , which is safely below the observed value (45). The octupole is suppressed by another three orders of magnitude. So, our model would serve as an alternative to other explanations [25, 27, 26, 28, 29, 30, 31] of the large dipole component of the CMB anisotropy, if such an explanation were needed (for observational aspects of this issue see Refs. [32, 33] and references therein).

## 6 Discussion

In this paper we have considered the effects on the anisotropy of CMB temperature due to possible tachyonic perturbations of dark energy. Because of the exponential growth, these perturbations may generate large gravitational potential  $\Phi$  at the recent cosmological epoch, and only at that epoch. This results in sizeable Sachs–Wolfe effect. Note that the tachyonic perturbations we have discussed are unrelated to perturbations in baryons or dark matter, so their contribution to the CMB anisotropy does not correlate with the distribution of structure in the Universe.

Our analysis was mostly motivated by the Lorentz-violating models of phantom energy. Hence, we have studied in detail the tachyonic perturbations with the dispersion relation (1). We have seen that their effect on the CMB angular spectrum has a pronounced maximum whose position depends on one of the parameters,  $\alpha$ , and is practically insensitive to the other parameter,  $M$ . It is expected that similar shape of the angular spectrum is characteristic to a wide class of models with Lorentz-violating tachyonic perturbations, as it is closely related to the fact that these perturbations become sizeable at late times only.

We have also considered tachyonic perturbations with Lorentz-invariant dispersion relation (2). In that case, the largest contribution to the CMB anisotropy is received by the dipole component, and the angular spectrum rapidly decays with the increase of  $l$ . We have seen that even if the observed dipole anisotropy is attributed to the tachyonic perturbations, the quadrupole component generated by them is still consistent with the observational data. It is worth noting that this result should be inherent not only in the Lorentz-invariant model, but also in Lorentz-violating models with tachyonic dispersion relations, provided that the “frequency” does not vanish at zero momentum and decreases as momentum increases.

Our main conclusion is that even if perturbations of the tachyonic type exist in the Universe, their contribution to the CMB anisotropy is small. Nevertheless, we do not exclude a possibility that growing precision of observations, and especially elaborate analysis of correlations between CMB anisotropy and structures in the Universe, may lead to hints towards the possible exotic property of dark energy, the tachyonic behaviour of its perturbations.

## Acknowledgements

This work has been partially supported by Russian Foundation for Basic Research grants 07-02-01034a (O.S. and M.S.) and 08-02-00473 (M.L. and V.R.), grant of the President of RF for leading scientific schools NS-1616.2008.2 (M.L. and V.R.), grant of the President of RF MK-2503.2008.2 (O.S.) and grant of Dynasty Foundation (M.L.) M.L. is indebted to Université Libre de Bruxelles, where part of this work has been done under partial support by the Belspo:IAP-VI/11 and IISN grants, for hospitality.

## References

- [1] T. Padmanabhan, Phys. Rept. **380** (2003) 235 [arXiv:hep-th/0212290].
- [2] V. Sahni, Lect. Notes Phys. **653** (2004) 141 [arXiv:astro-ph/0403324].
- [3] E. J. Copeland, M. Sami and S. Tsujikawa, Int. J. Mod. Phys. D **15** (2006) 1753 [arXiv:hep-th/0603057].
- [4] V. Sahni and A. Starobinsky, Int. J. Mod. Phys. D **15** (2006) 2105 [arXiv:astro-ph/0610026].
- [5] J. Frieman, M. Turner and D. Huterer, *Dark Energy and the Accelerating Universe*, arXiv:0803.0982 [astro-ph].
- [6] E. Komatsu *et al.* [WMAP Collaboration], *Five-Year Wilkinson Microwave Anisotropy Probe (WMAP) Observations: Cosmological Interpretation*, arXiv:0803.0547 [astro-ph].
- [7] V. Sahni, A. Shafieloo and A. A. Starobinsky, *Two new diagnostics of dark energy*, arXiv:0807.3548 [astro-ph].
- [8] J. Q. Xia, H. Li, G. B. Zhao and X. Zhang, *Determining Cosmological Parameters with Latest Observational Data*, arXiv:0807.3878 [astro-ph].
- [9] R. R. Caldwell, Phys. Lett. B **545**, 23 (2002)
- [10] L. Senatore, Phys. Rev. D **71**, 043512 (2005) [arXiv:astro-ph/0406187].
- [11] P. Creminelli, M. A. Luty, A. Nicolis and L. Senatore, JHEP **0612**, 080 (2006) [arXiv:hep-th/0606090].
- [12] V. A. Rubakov, Theor. Math. Phys. **149**, 1651 (2006) [Teor. Mat. Fiz. **149**, 409 (2006)] [arXiv:hep-th/0604153].
- [13] M. Libanov, V. Rubakov, E. Papantonopoulos, M. Sami and S. Tsujikawa, JCAP **0708**, 010 (2007) [arXiv:0704.1848 [hep-th]].
- [14] A. Sergienko, V. Rubakov, *Phantom dark energy with tachyonic instability: metric perturbations*, 2008 [arXiv:0803.3163 [hep-th]].
- [15] A.D. Linde, *Elementary Particle Physics and Inflationary Cosmology*, Moscow, “Nauka”, 1981.
- [16] A.D. Dolgov, Ya.B. Zeldovich, V.V. Sazhin, *Cosmology of the Early Universe*, Moscow State University Press, 1988.

- [17] V. Mukhanov *Physical Foundations of Cosmology*, Cambridge University Press, 2005.
- [18] M. R.olta *et al.* [WMAP Collaboration], *Five-Year Wilkinson Microwave Anisotropy Probe (WMAP) Observations: Angular Power Spectra*, arXiv:0803.0593 [astro-ph].
- [19] M. Giovannini, Int. J. Mod. Phys. D **14** (2005) 363 [arXiv:astro-ph/0412601].
- [20] I.S. Gradshteyn, I. M. Ryzhik, *Table of Integrals, Series, and Products*, Academic Press, 2000;  
M. Abramowitz and I.A. Stegun, *Handbook of Mathematical Functions with Formulas, Graphs, and Mathematical Tables*, New York, Dover, 1964.
- [21] [http://lambda.gsfc.nasa.gov/product/map/dr3/pow\\_tt\\_spec\\_get.cfm](http://lambda.gsfc.nasa.gov/product/map/dr3/pow_tt_spec_get.cfm)
- [22] [http://lambda.gsfc.nasa.gov/toolbox/tb\\_cmbfast\\_form.cfm](http://lambda.gsfc.nasa.gov/toolbox/tb_cmbfast_form.cfm)
- [23] J. Dunkley *et al.* [WMAP Collaboration], *Five-Year Wilkinson Microwave Anisotropy Probe (WMAP) Observations: Likelihoods and Parameters from the WMAP data*, arXiv:0803.0586 [astro-ph].
- [24] G. Hinshaw *et al.* [WMAP Collaboration], Astrophys. J. Suppl. **170** (2007) 288 [arXiv:astro-ph/0603451].
- [25] L.P. Grishchuk and Ya.B. Zeldovich, Sov. Astron. **22** (1978) 125.
- [26] B. Paczynski and T. Piran, Astroph. J. **364** (1990) 341.
- [27] M. S. Turner, Phys. Rev. D **44** (1991) 3737.
- [28] M. Jaroszynski and B. Paczynski, Astroph. J. **448** (1995) 448.
- [29] D. Langlois and T. Piran, Phys. Rev. D **53** (1996) 2908 [arXiv:astro-ph/9507094].
- [30] D. Langlois, Phys. Rev. D **54** (1996) 2447 [arXiv:gr-qc/9606066].
- [31] D. Langlois, Phys. Rev. D **55** (1997) 7389.
- [32] M. Kamionkowski and L. Knox, Phys. Rev. D **67** (2003) 063001 [arXiv:astro-ph/0210165].
- [33] C. Gordon, K. Land and A. Slosar, *Determining the motion of the solar system relative to the cosmic microwave background using type Ia supernovae*, arXiv:0711.4196 [astro-ph].